Acta Polytechnica **64**(6):582–587, 2024
https://doi.org/10.14311/AP.2024.64.0582

ANCHOR TEST AND LONG-TERM MONITORING OF GROUTED ANCHORS INSTRUMENTED WITH FIBER BRAGG GRATING SENSING TECHNOLOGY

Daniela Runczikováa[a,*], Jan Záleský[a], Marek Záleský[b], Jakub Koller[c], Ladislav Šašek[c]

[a] *Czech Technical University in Prague, Faculty of Civil Engineering, Department of Geotechnics, Thákurova 7, 166 29 Prague, Czech Republic*

[b] *SG Geotechnika a.s., Geologická 4, 152 00 Prague, Czech Republic*

[c] *SAFIBRA, s.r.o., U Sanitasu 1621, 251 01 Říčany, Czech Republic*

[*] corresponding author: daniela.runczikova@fsv.cvut.cz

Abstract. Geotechnical monitoring of anchors provides fundamental data for analysis and evaluation to ensure safe environment. The use of optic fiber sensing technology, especially Fiber Bragg Gratings, brings many advantages of optic fiber sensors, such as high measurement accuracy, real-time continual monitoring of deformation, on-line access to data and resistance against electromagnetic interferences. This article deals with anchor tests instrumented with FBG deformation gauges of the root and the tendon of the pre-stressed strand anchor in a test field in the Central Bohemian Region. First, the anchor with three optic cables with FBG sensors for measurement of axial deformation was subjected to six loading stages of the anchor test. Most of the sensors measured values of axial deformation less than 200 $\mu\varepsilon$ and the root mobilisation was observed. Then, the measurement continued by 26-day long-term monitoring and a trend of a small increase of deformations occurred.

Keywords: Fiber Bragg Gratings, anchor, geotechnical monitoring.

1. Introduction

Fiber optics provide a wide spectrum of applications, which include geotechnical health monitoring too, e.g. in foundation engineering (piles, anchors), slope stability monitoring (soil nails, monitoring of slope and subsoil deformation) and tunnel engineering (rock deformation, ground settlement), as summarised in [1–4]. One of the types of fiber optic sensing method is Fiber Bragg Grating (FBG), which belongs to the quasi-distributed optical sensing technology [3]. The Fiber Bragg Gratings (FBGs) in a optic fiber are created by exposition to ultraviolet light that changes refractive index [4, 5], and more recently by interference or phase mask methods [3–5]. FBG sensors are used to measure strain and temperature [6]. A change of a value of the measured quantity causes a shift of the wavelength of a reflected light of an appropriate sensor [3, 5, 6].

Some approaches to the use of FBGs for anchor monitoring are mentioned in [3], where sensors were glued into a groove of GFRP (Glass Fiber Reinforced Polymer) anti-floating anchor or installed in the GFRP anchor axial centre during a special production process and then pull-out tests were carried out [3]. In [7] FBG cables were used for monitoring of pull-out rock anchor test in the medium-hard rock mass of limestone quarry to investigate the stress distribution along anchors for anchor-grout and grout-rock interfaces. The cable was inserted in a longitudinal groove of an anchor or in a grout to measure the axial strain, but some of them failed before or during testing due to brittleness of cables [7]. Test of mobilisation of ground temporary anchor root resistance is described in [8], it took place in Prague in construction of a new extension of Grand Hotel Evropa and it was a previous version of anchor test described in this article.

2. Materials and methods

The measuring apparatus includes the monitoring unit FBGuard Mini equipped with 8 channels for strain and temperature sensing, it also includes an optical fiber with implemented FBGs elements covered with protective plastic tube and metal parts. Two test anchors with implemented FBGs elements for measurement of axial deformation were made in the factory hall and transported to the location of the anchor tests.

The anchor of the length of 12 m is marked K12 and the second one of 13 m long is labelled K13. A FBGs sensors distance was approximately 1 metre, the positions of the sensors on the anchors (centre of anchor and surface of anchor root) installed in the boreholes and a simple geological description of the subsoil are shown in Figure 1. The subsoil layer up to 0.3 m below the ground level consists of round-shaped gravel particles of variable size, the layer between 0.3 and 11.2 m consists of sandy gravel with cobbles of about decimetre size. An arkose was found below, first a yellow weathered arkose (up to 11.5 m), the next was a grey unweathered one [9]. The anchor tests took

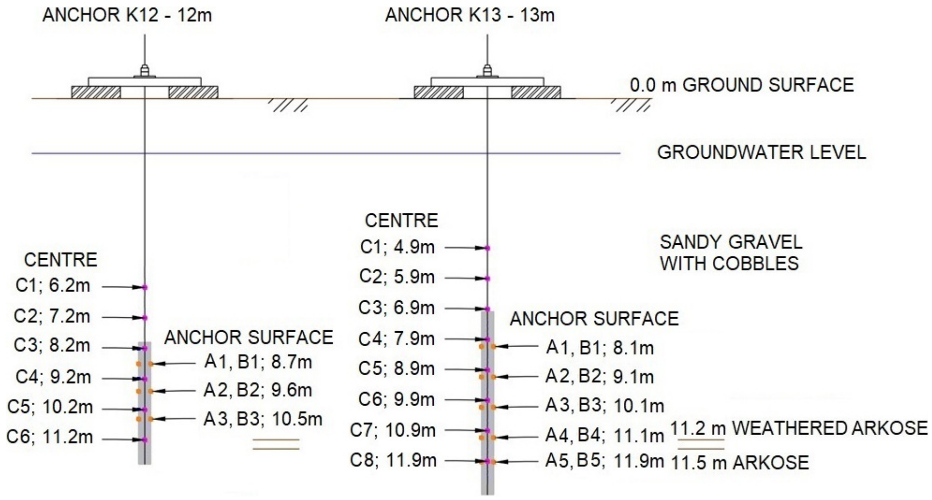

FIGURE 1. Positions of sensors and simple geological description of location [9].

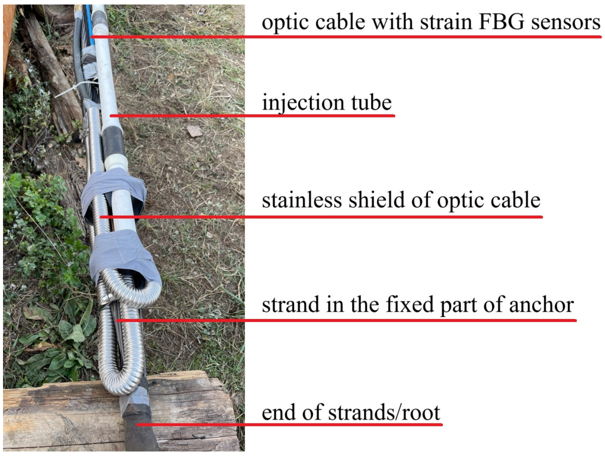

FIGURE 2. Lower part of the anchor root and protection of the redundant passive cable.

FIGURE 3. Loading bridge.

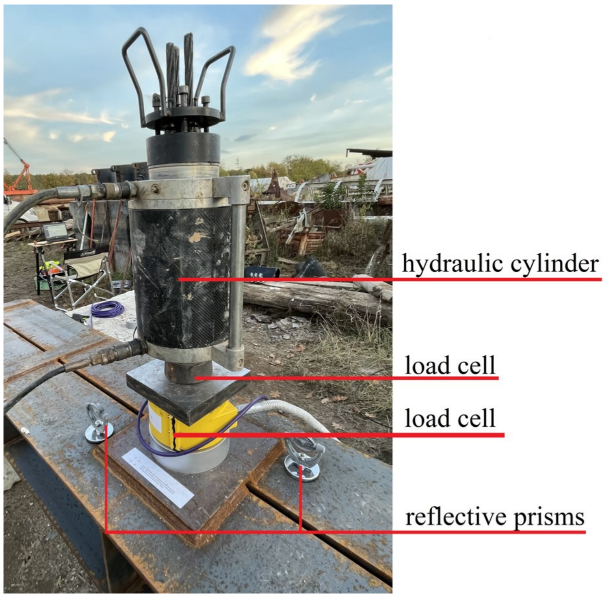

FIGURE 4. Monitoring assembly and pre-stressing system.

place near the village Staré Ouholice, which is a part of the cadastral territory Nové Ouholice, the municipality Nová Ves, the Mělník district in the Central Bohemian Region [10].

Two temporary test anchors were installed in the boreholes. The soil was compacted and aligned to horizontal ground level before drilling. At the time of soil compaction, a shallow softer inhomogeneity was discovered, which was removed and replaced by local sand. Two temporary vertical anchors (Figure 2) have high-pressure grouted roots, the length of the root of K12 is 4 m. In the case of K13, the root was extended to 6 m. Two pairs of concrete panels were placed on the ground as supports of the loading bridge (Figure 3). Two load cells were installed before the anchors were loaded. The first load cell was a part of the pre-stressing system. The second one (top-down description) was used for the loading test and for long-term monitoring of load and deformation development in the subsoil. Couples of reflective prisms were used for monitoring of the settlement of the bridge supports and the bridge beam deflection. Pair of prisms was mounted on opposite ends of the beam and the next pair was close to the bridge centre (Figure 4).

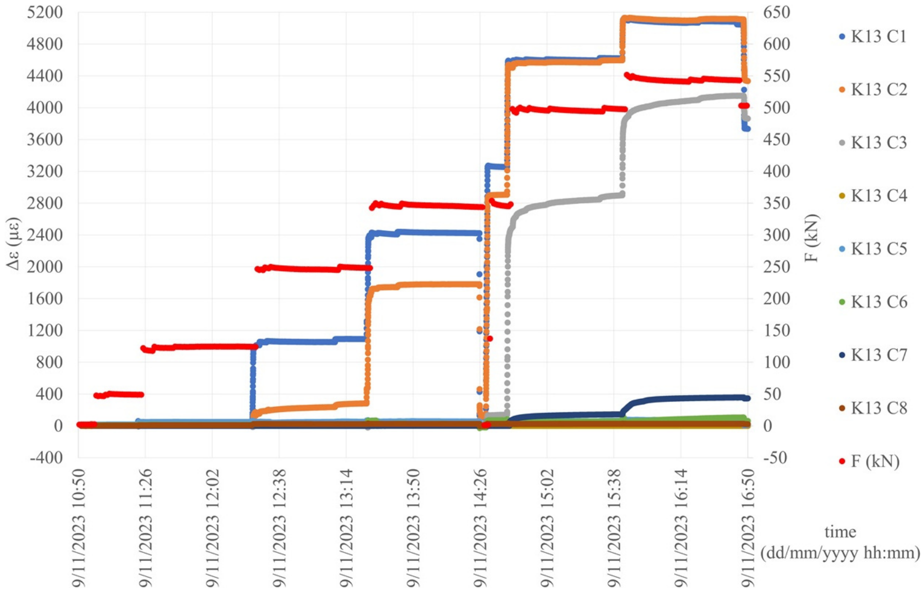

Figure 5. Graph of deformation of the sensors C1-C8 of the anchor K13 during test.

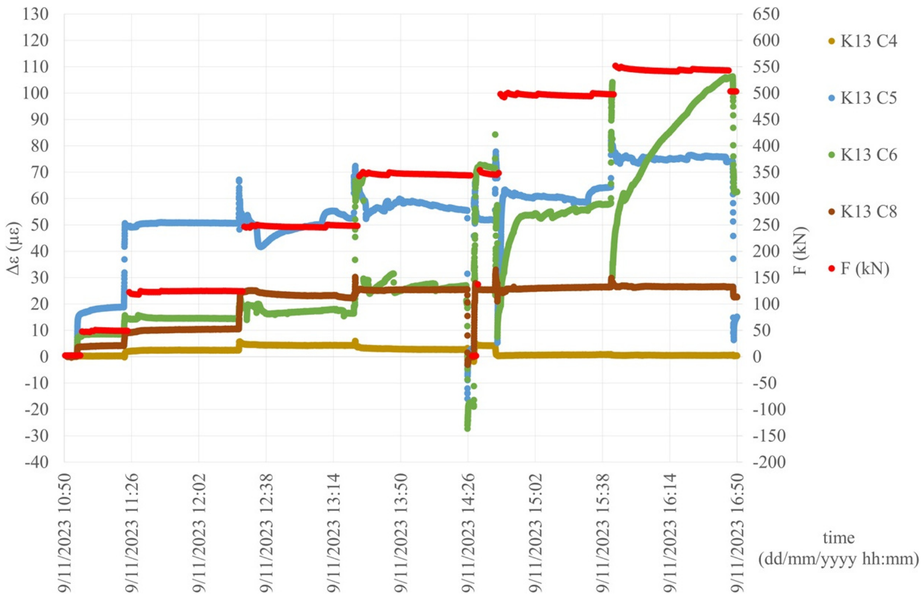

Figure 6. Graph of deformation of the sensors C4, C5, C6 and C8 of the anchor K13 during test.

The loading test of the anchor K12 took about six hours and in the case of the K13 was completed within six and a half hours. The anchor K12 was exposed to six loading stages (axial force 50 kN, 125 kN, 250 kN, 350 kN, 425 kN, 500 kN), the anchor K13 was loaded by six loading stages (50 kN, 125 kN, 250 kN, 350 kN, 500 kN, 550 kN). Each stage lasted at least 60 minutes and was considered complete when deformation of the tendon $\Delta s \leq \frac{0.1\,\text{mm}}{15\,\text{min}}$. The next monitoring of K12 took 7 days and 26 days in the case of K13.

3. Results and discussion

Results and discussion are presented for the anchor K13. The root of the anchor was on purpose extended up to 6 m to be sure to have a lower part of it not completely mobilised. The anchor K13 was instrumented by three parallel FBG sensing cables. The axial one is indicated by C and two same off-centre cables placed on the opposite sides of the anchor surface are labelled A and B (Figure 1). During the anchor test of K13 higher deformations (above 200 µε) of the sensors C1, C2, C3 and C7 were observed (Figure 5). The course of values of the sensors C1 and C2 are similar, especially for the fifth and the sixth loading stages. The values of the sensor C2 crossed the line of the sensor C1 during the sixth loading stage. Similarly, values of the sensor C7 exceeded the measured values of the sensors C4, C5, C6 and C8 after the fourth loading stage.

Very low deformation was recorded by the sensor C4 whose values moved near zero µε. The sensor C6 gathered similar values of deformation as the sensor C8 until the end of the fourth loading stage (Figure 6).

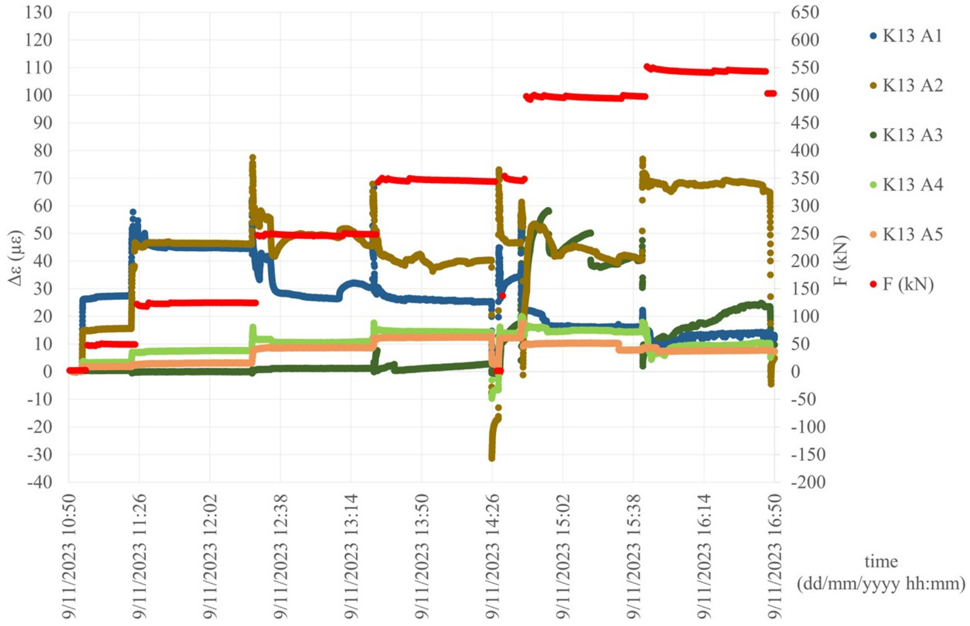

Figure 7. Graph of deformation of the sensors A1–A5 of the anchor K13 during test.

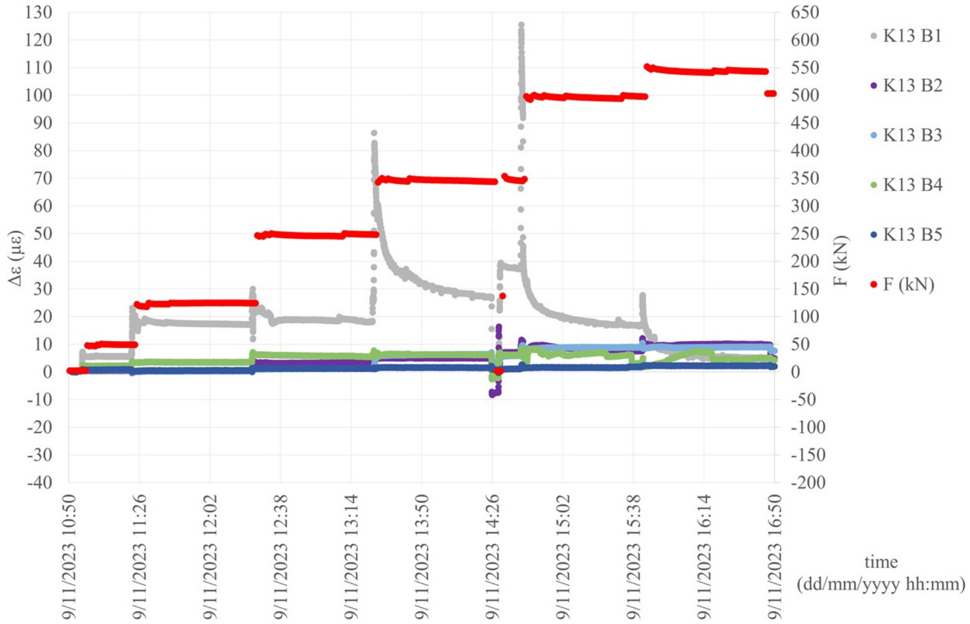

Figure 8. Graph of deformation of the sensors B1–B5 of the anchor K13 during test.

The next loading stages and the disproportional increase of values along the centre of the anchor root towards the root lower end was caused with very high probability by nonuniform penetration of the cement grout during the high pressure injection carried out in stages.

The sensors on the surface of the anchor root measured low deformation. After the second loading stage, the values of the sensor A1 were mainly decreasing and exceeding the values of the sensor A2. On the contrary, the sensor A3 had deformation near zero $\mu\varepsilon$ at the beginning, then its values were higher and closer to the sensor A2, but during the sixth loading stage they fell off closer to the sensors A1, A4 and A5 (Figure 7).

The sensors B1–B5 of the anchor root surface measured very small deformations, except for the sensor B1 with a maximum of over 120 $\mu\varepsilon$. The local maxima of the sensor B1 occurred during transition between loading stages that were also observed in the courses of other sensors, e.g. A1, A2, A4 and C5 (Figure 8).

During long-term monitoring the deformation measured by the sensors C1, C2 and C3 is decreasing (Figure 9). On the contrary, values of the sensor C6 increased steeply at the beginning of the long-term monitoring (during the first 31 hours) and then were practically constant. This was probably caused by consolidation of the soil after the change of loading in the subsoil due to anchor tension. The course of deformation of the sensor C7 gradually increased. An

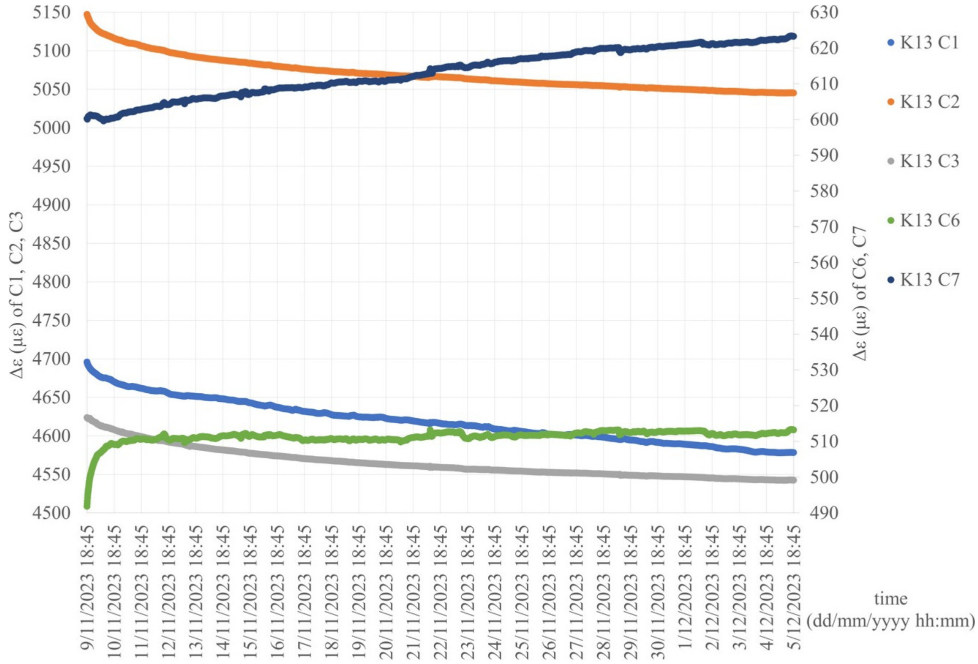

FIGURE 9. Graph of deformation of the sensors C1, C2, C3, C6, C7 of the anchor K13 during long-term monitoring.

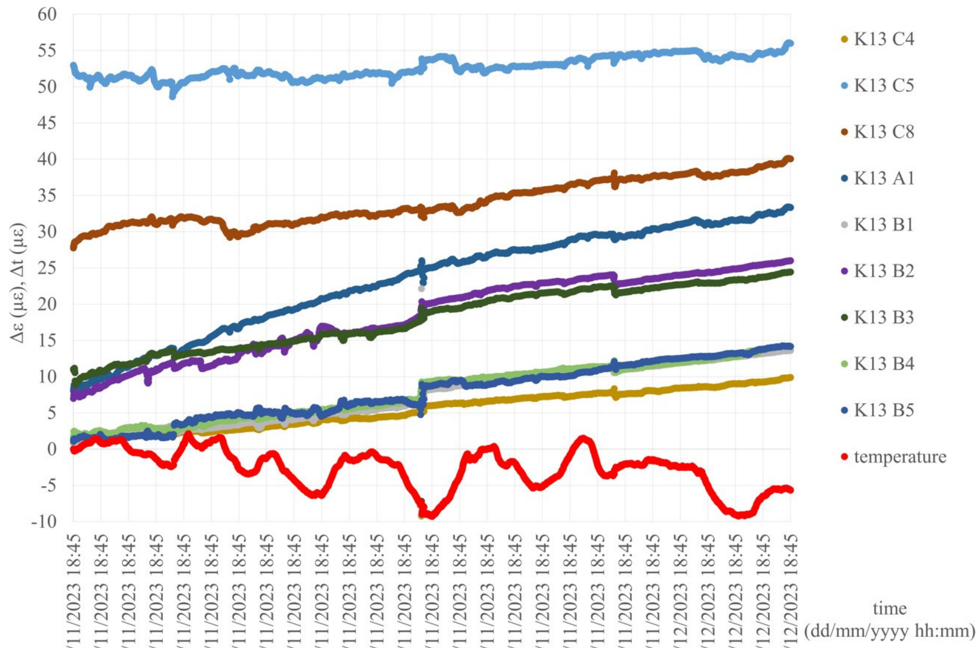

FIGURE 10. Graph of temperature and of deformation of the sensors C4, C5, C8, A1 and B1–B5 of the anchor K13 during long-term monitoring.

increasing trend of deformation can also be observed in the measurements of the other sensors (Figure 10).

From the graphs it is apparent that some sensors exceeded values in an unexpected order. The high pressure grouting did not produce "a root of a constant diameter cylinder" but more complicated and irregularly shaped root body due to the stratified soil sequence and arkose at the root end. These effects resulted in not uniformly dissipating strain along the root towards its end. That can be seen as a positive in terms of the pull-out resistance of the anchor from the host mass.

4. CONCLUSION

The article deals with the testing of Fiber Bragg Grating (FBG) sensors applied to grouted strand anchors. Measurements with FBG sensors provided an adequate view of an anchor root mobilisation process. The new FBG system has been successfully applied for short- and long-term monitoring of the anchor axial deformation in front of and along the whole length of the root. The dependence of the measured data on temperature was insignificant in this case due to the approximately constant ambient temperature.

For further development, adjustments of design for routine use and a possible modification of the FBG-based sensor for winding of equipped anchors on transport coils are also being considered.

Acknowledgements

The presented part of the research was supported by the project No. FW01010384 “Development of fibre optic measurement instruments for underground constructions and retaining structures” funded by the Technology Agency of the Czech Republic. The gathered data were used for new analyses and evaluation supported by the project SGS24/042/OHK1/1T/11 “Application of fiber optic sensor FBGI for monitoring of slope movement in boreholes” of the Grant Agency of the Czech Technical University in Prague.

References

[1] C.-Y. Hong, Y.-F. Zhang, M.-X. Zhang, et al. Application of FBG sensors for geotechnical health monitoring, a review of sensor design, implementation methods and packaging techniques. *Sensors and Actuators A: Physical* **244**:184–197, 2016. https://doi.org/10.1016/j.sna.2016.04.033

[2] Y. Zheng, Z.-W. Zhu, W. Xiao, Q.-X. Deng. Review of fiber optic sensors in geotechnical health monitoring. *Optical Fiber Technology* **54**:102127, 2020. https://doi.org/10.1016/j.yofte.2019.102127

[3] J. Ma, H. Pei, H. Zhu, et al. A review of previous studies on the applications of fiber optic sensing technologies in geotechnical monitoring. *Rock Mechanics Bulletin* **2**(1):100021, 2023. https://doi.org/10.1016/j.rockmb.2022.100021

[4] M. J. Singh, S. Choudhary, W.-B. Chen, et al. Applications of fibre Bragg grating sensors for monitoring geotechnical structures: A comprehensive review. *Measurement* **218**:113171, 2023. https://doi.org/10.1016/j.measurement.2023.113171

[5] Y. Yao, M. Yan, Y. Bao. Measurement of cable forces for automated monitoring of engineering structures using fiber optic sensors: A review. *Automation in Construction* **126**:103687, 2021. https://doi.org/10.1016/j.autcon.2021.103687

[6] B. G. Lipták (ed.). *Instrument Engineers’ Handbook: Process Measurement and Analysis*, vol. 1. CRC PRESS Taylor and Francis Group, 4th edn., 2003. https://doi.org/10.1201/9781420064025

[7] B. Grindheim, C. C. Li, A. H. Høien. Full-scale pullout tests of rock anchors in a limestone quarry focusing on bond failure at the anchor-grout and grout-rock interfaces. *Journal of Rock Mechanics and Geotechnical Engineering* **15**(9):2264–2279, 2023. https://doi.org/10.1016/j.jrmge.2023.04.002

[8] K. Čápová. *Use of optical fibres for deformation monitoring in geotechnics*. Ph.D. thesis, Czech Technical University in Prague, Faculty of Civil Engineering, 2020.

[9] Czech Geological Survey. Statement of borehole ID 205603 from database of the geologically documented objects in the Czech Republic, 2023.

[10] State Administration of Land Surveying and Cadastre. Nové Ouholice. [2023-02-22]. https://www.cuzk.cz/Dokument.aspx?AKCE=META:SESTAVA:MDR002_XSLT:WEBCUZK_ID:706582